

## Oxidation in catalytic membrane reactors

Jean-Alain Dalmon, Arquimedes Cruz-López, David Farrusseng, Nolven Guilhaume, Eduard Iojoiu, Jean-Christophe Jalibert, Sylvain Miachon\*, Claude Mirodatos, Amalia Pantazidis, Michael Rebeilleau-Dassonneville, Yves Schuurman, Andre C. van Veen

*Institut de Recherches sur la Catalyse et l'Environnement de Lyon (IRCELYON), UMR5256 CNRS/Université Claude Bernard Lyon 1, 2 avenue A. Einstein, 69629 Villeurbanne Cedex, France*

Available online 30 March 2007

### Abstract

This paper presents a series of applications of catalytic membrane reactors (CMR) to oxidation reactions. Four reactions were tested in our group. Alkane activation (C2, C3 and C4) or total oxidation (WAO) is implemented in various membrane reactor modes, using dense, microporous or mesoporous membranes. In some cases, a catalyst bed is associated with a membrane, whereas other applications use an intrinsically active membrane. Progresses in catalyst and membrane design, along with careful operational conditions led to overall higher performances when compared to conventional processes.

© 2007 Elsevier B.V. All rights reserved.

**Keywords:** Oxidation; Oxidative dehydrogenation; Wet air oxidation; Catalytic membrane reactors

### 1. Introduction

Oxidation reactions form an important class of catalytic processes that play a key role in numerous industrial and environment-related applications. Either selectivity (partial and selective oxidation) or conversion (pollution remediation) may be the main concern in oxidation processes. Beside catalyst formulation, adapted reactor design is often considered as a way to improve process performance.

Among innovative reactors, structured systems are subject of intensive R&D efforts. Catalytic membrane reactors (CMR) [1] are structured reactors combining in a single unit a membrane controlling mass transfers, and a catalyst providing chemical activity [2].

There are different types of CMRs [2], among which the *extractor* type is the most commonly studied. In this case, the membrane is used to selectively extract reaction products from the catalyst bed. It is particularly well suited to favour conversion (equilibrium-restricted reactions) or selectivity (selective extraction of a primary product in consecutive reactions). Our group have studied other configurations than extractors, where the

membrane, still embedded into the catalytic reactor, plays a different role. In all cases, these systems can be well adapted to oxidation or oxidative dehydrogenation reactions that have been less studied in CMRs [3–9].

*Distributor* CMRs are set-ups where the membrane is used to feed one of the reactants to the catalyst bed, in a way that proves an advantage for the applications. Two examples are given in this paper. Selective oxidation of butane to maleic anhydride was carried out with a membrane used to homogeneously feed oxygen to the catalyst bed. This allowed operation under conditions that are forbidden, for safety reasons, with conventional co-feed, while retaining a high selectivity. Oxidative dehydrogenation of propane uses a membrane also for oxygen distribution. In this case, the purpose is to control oxygen partial pressure, in order to increase the selectivity towards the targeted product (propene).

Applications of *high temperature oxygen-permselective membranes* to oxidative dehydrogenation of light hydrocarbons utilise a different membrane property: its ability to feed activated oxygen species to the catalyst, leading to a different catalytic behaviour than under conventional hydrocarbon/oxygen co-fed operations.

In a completely different mode, *interfacial contactor* CMRs take advantage of the unique catalytic membrane geometry. Here the membrane is also catalytically active, providing two

\* Corresponding author. Tel.: +33 4 72 44 53 84; fax: +33 4 72 44 53 99.  
E-mail address: [Sylvain.Miachon@ircelyon.univ-lyon1.fr](mailto:Sylvain.Miachon@ircelyon.univ-lyon1.fr) (S. Miachon).

ways to reach the catalyst. Reactants are thus admitted separately from both sides of the membrane, allowing the reaction to proceed into the membrane wall. This configuration leads to much better contact between the two reactant phases and the catalyst. This will be illustrated in the last part of this paper, in the case of wet air oxidation of water pollutants. Thus, this contribution intends to present some typical configurations of catalytic membrane reactors applied to catalytic oxidation reactions. However, it is not meant to be a full literature review of this subject.

## 2. Selective oxidation of butane to maleic anhydride

Maleic anhydride production by butane partial oxidation is a common process in industry. This catalytic process may even be the only important one converting directly an alkane into oxygenated product. The catalyst used for this process is a VPO-based material [10]. They offer high selectivity towards maleic anhydride together with high butane conversion. However, the flammability limits of the butane–air mixture restricts butane concentrations to very low values (typically 2 vol.%). Moreover, the possibility of hot spots in the fixed catalyst bed configuration, and catalyst attrition problems in fluidized beds, can bring major difficulties. In this prospect, the distribution of oxygen along a fixed bed of catalyst can provide an answer to both drawbacks [11,12].

Here, VPO-based catalysts, especially adapted to highly reducing conditions, are combined with a microporous zeolite-alumina nanocomposite membrane [13] to operate this reaction with a higher feed flux of butane to the catalyst.

### 2.1. Catalyst

Co-doped VPO catalysts were prepared via the *organic route* [14], using cobalt acetate, phosphoric acid and vanadium pentoxide precursors [15], with a Co/V ratio of 3%. Standard VPO catalyst was prepared in the same way for comparison purposes. The catalyst was then activated under reaction conditions (1.5% butane in air at 470 °C) for 72 h.

### 2.2. Membrane

An MFI based membrane, presenting a nanocomposite structure within a porous alumina tube, was used. The tube was 15 cm long (13 cm used length, 1 cm enamel endings), 1 cm external diameter, and 1.5 mm thick. This support was submitted to hydrothermal synthesis conditions in a 3-day aged precursor solution of silica (Aerosil 380) and tetrapropylammonium hydroxide). The material was then calcined in air at 773 K for 3 days.

The resulting MFI/alumina membrane was tested for defect using a butane/hydrogen gas mixture separation at room temperature [16]. It offered an equivalent thickness of about 5  $\mu\text{m}$ . More details on the preparation and membrane structure can be found elsewhere [13].

### 2.3. Reactor and testing

A stainless steel module, equipped with graphite fittings, was used to mount the membrane, in the lumen of which was packed 2.5 g of catalyst, diluted 3:1 in quartz. The temperature profile was measured along the axis of the membrane tube (internally), and was homogeneous within more or less 8 °C for a nominal value of 400 °C. The reactor could be fed both through the membrane from the outer compartment (oxygen) and directly into the inner compartment (butane). Both oxygen and butane (1.2–22 kPa) were diluted in helium, and fed through mass flow controllers for an overall oxygen/butane ratio of 0.5–12 and a GHSV varying from 15 to 180  $\text{h}^{-1}$ . A differential manometer, a regulator and an automatic valve connected to the outlet if the inner compartment was used to regulate the pressure difference across the membrane, in order to allow the desired oxygen flux through the membrane to the catalyst bed. The reactor outlet stream was analysed on line, using gas chromatography (FID & TCD). More details on the set-up can be found in Ref. [15].

In this work, the catalytic performance is mainly expressed in terms of volumetric productivity (with respect to the catalyst bed volume).

### 2.4. Catalyst adaptation to membrane reactor conditions

Due to the distributor effect, there is a continuous change of oxygen/butane ratio along the catalyst bed. Therefore, the VPO-based catalyst used for this work was adapted to the low oxygen/butane ratio present at the inlet of the catalyst bed (reducing conditions). The addition of Co proved quite efficient in this purpose, as can be seen on Fig. 1.

The reason why this formulation keeps such a high maleic anhydride selectivity over the whole oxygen/butane ratio range (and particularly at low values of this parameter) can be examined in the following way.  $\text{V}^{4+}$  species on themselves favour butane oxidative dehydrogenation, whereas in presence of  $\text{V}^{5+}$  only, total oxidation is favoured. The formation of maleic anhydride necessitates both oxidation states of vanadium [17].

Spin-echo mapping NMR previously showed the role of Co in the stabilisation of  $\text{V}^{5+}$  species in reducing conditions [14]. The substitution of  $\text{V}^{4+}$  by  $\text{Co}^{2+}$  is charge-balanced by a  $\text{V}^{5+}\text{O}^-$

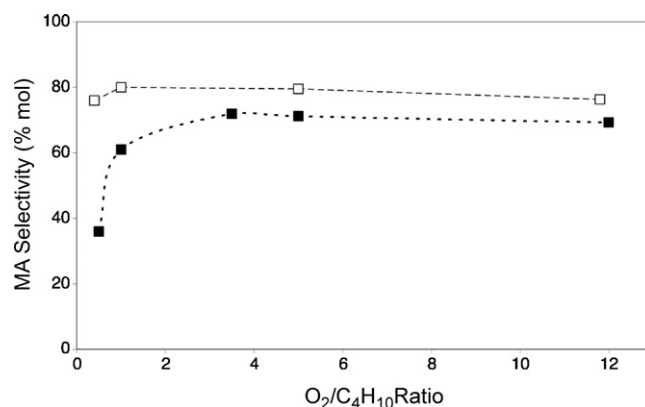


Fig. 1. Maleic anhydride selectivity as a function of the oxygen/butane ratio. Black symbols: VPO catalyst, white symbols: 3%Co/CPO catalyst.

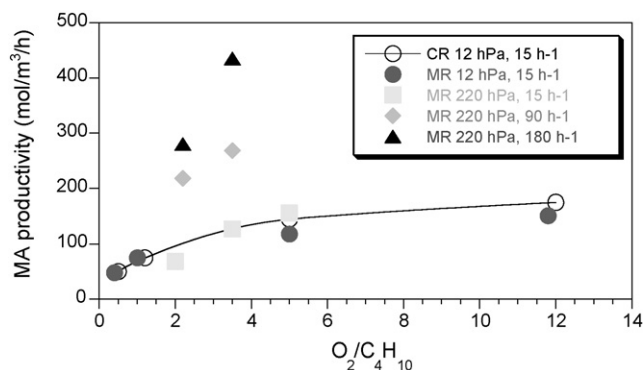


Fig. 2. Comparison of maleic anhydride productivity as a function of the global oxygen/butane ratio on 3%CoVPO in the conventional fixed-bed Reactor (CR) and membrane reactor (MR).

group (instead of  $V^{4+}=O$ ), leading to a stable catalytic site in reducing conditions. Moreover,  $Co^{2+}$  is the only divalent cation small and stable enough to play this role [18].

### 2.5. Catalytic membrane reactor performance

Fig. 2 shows the compared productivity of a conventional fixed-bed reactor and a membrane reactor using the same catalyst. In similar conditions, both offer similar performances. However, the CMR allows higher feed butane partial pressure operation, leading to a large increase in maleic anhydride productivity at low oxygen/butane ratio.

This result shows that with an adapted catalyst formulation, a *distributor* CMR offers interesting improvement for partial oxidation productivity. This is due to the fact the reactor is operating globally within the flammability zone, while keeping local mixture compositions out of it in any point of the catalyst bed.

To go further, a benefit could be drawn from the change of the oxidizing character of the gas mixture along the catalyst bed. This leads to a progressive gradient of the catalyst oxidation state, being over-reduced at the inlet (hydrocarbon feed) and over-oxidized at the outlet. By reversing the butane feed stream, it has been observed a transient state of maleic anhydride over-production, due to the locally accumulated oxygen species inside the VPO catalyst [2]. By cycling this reversal, one can imagine to further increase the productivity of the system.

## 3. Oxidative dehydrogenation of propane

The oxidative dehydrogenation of alkanes to olefins is a promising alternative to conventional non-oxidative cracking processes (cheap available feedstocks and no coke formation). However, it still suffers from yield limitation due to  $CO_x$  formation. Thus, for the oxidative dehydrogenation of propane (ODHP), a maximum yield towards propene of about 15% is obtained under steady-state conditions (when oxygen is co-fed with hydrocarbon) with the best identified systems like VMgO catalysts [19–21]. This limitation comes from a Mars–van Krevelen mechanism implying surface and bulk reactions with competing selective and non-selective steps [22,23]. Similar

conclusions were achieved for the case of oxidative dehydrogenation of butane (ODHB) [24].

Among the various ways attempted to improve the yield in alkene, two were thoroughly investigated in our laboratory, based on the statement that a reducing environment enhances the dehydrogenation reaction at the expenses of the total combustion: (i) using membrane reactor as a *distributor* to get a better control of oxygen concentration along the catalyst bed, (ii) running the ODH process under non-steady-state conditions in order to favour the selective routes.

### 3.1. Catalytic membrane reactor for ODHP

As mentioned in Section 1, catalytic membrane reactors can be set up in different ways. In a first study [25], various contactor modes were tested. For this purpose, several MFI membranes, including modifications, were prepared. However, no positive effect was observed in comparison to conventional fixed-bed processes.

In another approach the reaction was carried out in a *distributor* CMR. In this case, a tubular zeolite membrane, similar to that previously described, was used as an oxygen distributor to feed, in a controlled way, a VMgO catalyst fixed bed enclosed in the inner compartment. The purpose here is to limit the local oxygen concentration on the catalyst, in order to favour the alkene production.

The catalytic performance of this reactor was compared to that of an equivalent fixed-bed system. Fig. 3 shows the data obtained at 500 °C while varying the  $P_{(C_3H_8)}/P_{(O_2)}$  ratio from 1:0.66 to 1:8, and the feed flow from 100 to 20 ml min<sup>-1</sup>.

Over the whole conversion range, propene selectivity in the CMR is constantly above the values obtained in the conventional reactor, by 15–80% in relative values at similar conversions. This allows reaching propene yields up to 15%. However, this positive effect was less important at higher propane conversions, obtained at high oxygen pressures. The trans-membrane pressure gradient  $\Delta P$  was also found to influence propene selectivity and yield: at high oxygen partial pressure ( $P_{(C_3H_8)}/P_{(O_2)} = 1 : 8$ ), the propene yield increased from 12 to 16% when decreasing the  $\Delta P$ .

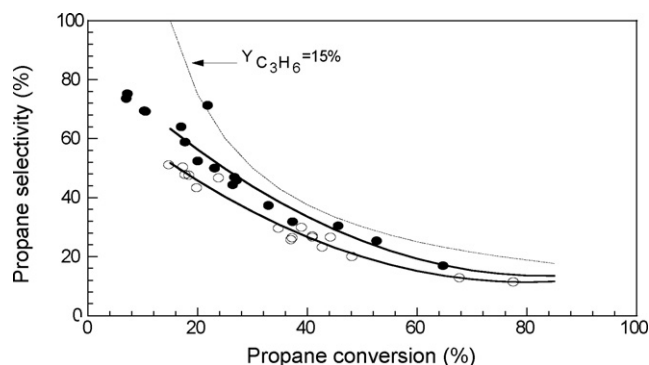


Fig. 3. Propene selectivity vs. propane conversion at 500 °C for the hybrid membrane reactor; full marks: separate feeds with  $C_3H_8$  at the inner compartment (distributor mode), empty marks: co-feed (conventional fixed bed); iso-yield at 15%.

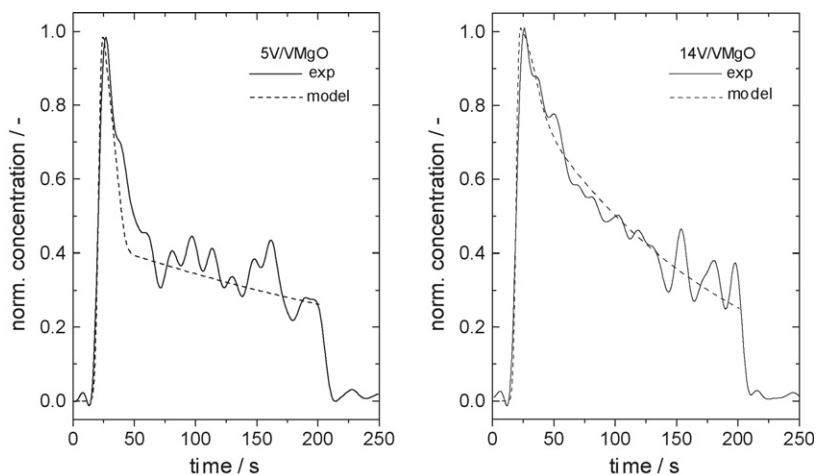


Fig. 4. Response signals for  $C_3H_6$  in a step transient of propane over a: (i) 5V/VMgO and a (ii) 14V/VMgO catalyst (solid line: experimental; dashed line: simplified model based on the existence of two distinct pools of oxygen, bulk and surface) [27].

This could be due to a higher oxygen flux through the membrane with a negative impact on propene selectivity. In this *distributor* configuration, oxygen permeates all along the zeolite membrane onto the catalyst bed, and propane consumes practically all the diffused oxygen in the dehydrogenation reaction. This gradual permeance of oxygen through the membrane permits high  $C_3H_8/O_2$  ratios, thus enhancing propene selectivity.

As reducing atmospheres are proven to favour ODHP, we also explored another way to keep a controlled oxidation state of the catalyst: non-stationary operation using the same VMgO catalyst.

### 3.2. ODHP dynamics: step transients experiments

From the known statement that higher yield and selectivity can be obtained in anaerobic transient operation mode [26,27], we demonstrated in Ref. [27] how transient in situ electrical conductivity experiments combined with transient kinetic studies lead to improved understanding of the mechanism and allowed us to determine kinetic parameters required for any scale-up of ODHP in the non-steady-state regime. The evolution of electric conductivity of VMgO catalysts in presence of propane allowed to show surface and bulk effects corresponding to surface reaction and bulk oxygen species diffusion.

As illustrated in Fig. 4, during an anaerobic step transient, a significant propene production can be obtained initially, depending on the nature of the catalysts such as the concentration of V [27]. The propene yield can then reach 20%, which is even higher than steady state operation in the *distributor* membrane reactor (15%). However, this advantage of the transient operation vanishes for time of exposure to propane longer than ca. 2 min. In a process where the catalytic phase (in a fixed-bed or in a membrane reactor) would be alternatively contacted with pure propane and then regenerated under air flux, this time limit would correspond to the anaerobic sequence.

By modelling these transient responses, all kinetic parameters (rate constants, diffusion constants, amount of reactive oxygen available) were also derived. More details about the model can be found in Ref. [27].

Comparing the performances obtained for ODHP over VMgO catalysts either in a conventional fixed-bed reactor, in the *distributor* membrane reactor, or under transient operating conditions, it was demonstrated that non-steady-state experiments improve significantly propene yields, as compared to steady-state operations, either in fixed-bed or in the membrane reactor. Combining the positive aspects of all these tested configurations might lead to further yield improvement.

## 4. Oxidative dehydrogenation of ethane

Although promising catalyst formulations have been recently discovered for ODHE, their performances in terms of ethylene space time yield are well below commercial requirements. The best activity reported so far is  $0.06 \text{ ml } C_2H_4 \text{ min}^{-1} \text{ g}^{-1}$  for NiTaNb oxides [28]. In this context, dense ionic oxygen conducting membrane reactors (IOCMR) are highly attractive solutions, where both separation and reaction are integrated in a same unit. As depicted in Fig. 5, the IOCMR supplies activated

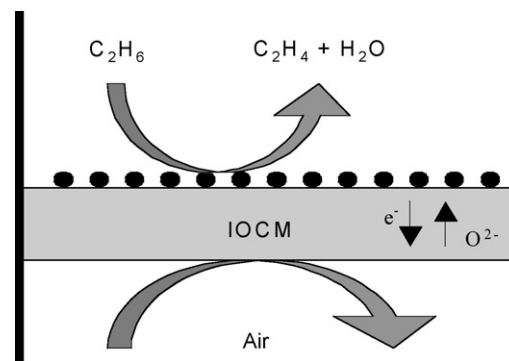


Fig. 5. Reactor scheme for the oxidative dehydrogenation of ethane using surface modified dense membrane with electronic and ionic conductivity properties.

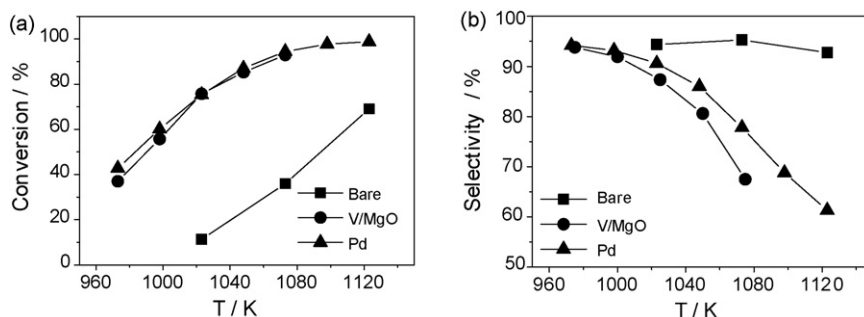


Fig. 6. Ethane conversion (a) and ethylene selectivity (b) as a function of temperature, for different modified membranes. Total feed to the reaction side of  $37 \text{ ml min}^{-1}$  at  $P_{(\text{ethane})}/P_{\text{O}} = 0.255$ .

oxygen to the reaction compartment by permeation through the solid phase ensuring herewith an efficient and selective separation from air fed to the second compartment. Recently, Wang et al. have reported a per pass ethylene yield of 67.4% ( $S = 80\%$ ) using a perovskite structured  $\text{Ba}_{0.5}\text{Sr}_{0.5}\text{Co}_{0.8}\text{Fe}_{0.2}\text{O}_{3-\delta}$  (BSCFO) IOCM [29,30] at 1073 K. In this part we report on the concept and implementation of membrane surface modifications [31] by deposition of micro particles enabling to improve the reactivity and increase the concentration of active sites by several order of magnitudes (Fig. 6).

The membrane support is a dense BSCFO perovskite disc of 1 cm in diameter and 1 mm thickness exhibiting high oxygen permeability, as described previously [32,33]. A detailed synthesis procedure is given in Ref. [34]. Its modification was carried out by two different ways: (i) the deposition of a metal phase by a laser vaporization technique [35] which yields an excellent dispersion of Pd nano-clusters and a coverage of about 10% of the area, (ii) the deposition of a very thin layer of VMgO catalyst by spin casting technique yielding to a loading of about 1 mg of V/MgO per  $\text{cm}^2$ .

Experiments were performed using a membrane reactor as described in Ref. [34]. The air side was fed at constant total pressure of 120 kPa with a total flow of  $50 \text{ ml min}^{-1}$  synthetic air. For oxygen permeation studies a flow of  $35 \text{ ml min}^{-1}$  He is used as a sweep gas whereas for ODHE studies the reaction side was fed with ethane diluted in helium. A significant enhancement in oxygen permeability was observed after the V/MgO membrane surface modification, whereas Pd clusters improved the membrane performance to a minor extent. Under ODHE conditions, the catalytic performances of the unmodified membrane in terms of selectivity and conversion over the whole range of temperature matches well with data in other studies [29,30]. Noteworthy, no oxygen was observed in gas phase and the selectivity to carbon oxides was always lower than 5%.

Both samples with surface modifications (Pd and VMgO) showed an outstanding rise in conversion while selectivity remained high [36]. At 1020 K, conversion increased by a factor of 8. The maximum yield in ethylene reached 73% for V/MgO and 75% for Pd at 1050 K at an ethylene selectivity of 80 and 86%, respectively. Carbon containing by-products are mainly CO and  $\text{CO}_2$  with some traces of methane.

As in the case of the unmodified membrane, neither oxygen was detected in the effluent nor coke (usually associated with

thermal cracking) was formed during several days of use. It is believed that part of the oxygen crossing the BSCFO membrane reacts as activated species ( $\text{O}^{2-}$ ,  $\text{O}^-$ , or  $\text{O}_2^-$ ) with hydrogen depleted adsorbed  $\text{C}_2\text{H}_y$  species before they can polymerize, thus preventing any coke formation. In addition, a large portion of hydrogen (up to 80% of the ethylene content) indicates that direct dehydrogenation of ethane occurs considerably in parallel to ODHE.

In conclusion, the use of IOCMRs provides a real alternative to conventional thermal dehydrogenation. A synergy between oxygen permeation and catalytic oxidation at the membrane surface is assumed to be responsible for the observed outstanding performance. On the other hand, it is demonstrated that catalytic surface modifications allow to decouple oxygen supply features of a bulk material from the fine tuning of catalytic entities at the surface. This concept opens new perspectives in advanced catalysis for several reactions proceeding according to the Mars and van Krevelen mechanism.

## 5. Wet air oxidation

Wet air oxidation is a major process for waste water treatment. It is usually carried out at high temperatures in conventional reactors either in non-catalytic processes or using a homogenous catalyst. The *Watercatox* process (catalytic wet air oxidation of wastewater) is based on an interfacial gas-liquid contactor hosting a porous ceramic membrane containing heterogeneous catalyst nano-particles in the top layer [37]. The synergy of the catalyst and the membrane, when implemented in the same device, was decisive in the improvement of the catalytic performance that clearly overtakes the performances of a conventional CSTR configuration [38].

In the interfacial contactor mode, the gas and the liquid phases are separately introduced within the membrane from opposite sites. The gas-liquid interface is then located within the membrane, its location being controlled by the trans-membrane differential pressure that compensates for the gas-liquid capillary forces within the membrane pores [39]. The contactor catalytic membrane reactor (CMR) is known to favour the triple contact between two different reactant fluid phases and the catalyst, the reactants exhibiting a better accessibility to the catalyst particles which leads to a significant improvement of the conversion rates [40,41].

Table 1  
Porous structure of the ceramic membrane types used in this work

Structure	Membrane ref. (provider)		
	a/A (Pall Exekia)	b/B (Pall Exekia)	c/C (Inocermic)
<b>Top-layer</b>			
Composition	ZrO <sub>2</sub>	ZrO <sub>2</sub>	CeO <sub>2</sub> /ZrO <sub>2</sub>
Pore size	50 nm	20 nm	~80 nm
<b>1st intermediate layer</b>			
Composition	–	TiO <sub>2</sub> -covered α-Al <sub>2</sub> O <sub>3</sub>	TiO <sub>2</sub>
Pore size		0.2 μm	0.25 μm
<b>2nd intermediate layer</b>			
Composition	TiO <sub>2</sub> -covered α-Al <sub>2</sub> O <sub>3</sub>	TiO <sub>2</sub> -covered α-Al <sub>2</sub> O <sub>3</sub>	TiO <sub>2</sub>
Pore size	0.8 μm	0.8 μm	0.8 μm
<b>Support</b>			
Composition	TiO <sub>2</sub> -covered α-Al <sub>2</sub> O <sub>3</sub>	TiO <sub>2</sub> -covered α-Al <sub>2</sub> O <sub>3</sub>	TiO <sub>2</sub>
Pore size	12 μm	12 μm	5 μm

Capitals indicate multichannel systems, and lower case letters indicate single tubes.

### 5.1. Catalytic membranes

Catalyst supports were ceramic membranes, provided by Pall Exekia (France) and Inocermic (Germany). Single tube membranes were designed and developed for lab-scale tests (10 mm external diameter, 7 mm internal diameter and 250 mm length). Especially developed multichannel systems have been used for further tests, including real industrial effluent oxidation. Two geometries have been used: hexagonal (Pall Exekia) of 31.5-mm diagonal, 250 mm-long providing 37 channels of 3-mm diameter, and cylindrical (Inocermic) of 25 mm diameter, 250 mm-long, providing 19 channels of 3.3 mm. Both membrane endings have been covered with enamel or glaze in order to achieve a proper sealing and soften the surface where adapted rubber seals were applied. The materials were made of three or four concentric layers, showing an average pore size decreasing from the outside to the internal surface of the channel, the top layer being located on the inner surface of the channels (Table 1). Pure alumina supports were excluded, due to their limited chemical resistance to the present acidic effluents [37].

The catalytic performance depending strongly on the loading and location of the platinum catalyst, the preparation procedure was adapted to achieve a controlled deposition closer to the toplayer of the ceramic support. The catalyst deposition was carried out using an evaporation–crystallization technique. Further details can be found in Ref. [42].

### 5.2. Reactor set-up and operation

The catalytic membrane was mounted in a module using a tight seal separating the liquid and gas feeds. The liquid phase was introduced on the inner side of the tube and was maintained close to the atmospheric pressure, while the gas phase was fed on the shell side. The gas overpressure was monitored and

carefully controlled by the way of the gas feed flow (50 ml min<sup>-1</sup> for single tubes and 500 ml min<sup>-1</sup> for multi-channels). According to Laplace law on capillary pressure, the gas–liquid interface can be displaced from the support zone towards the top layer, where the catalyst is concentrated, by increasing the gas overpressure [39].

The membrane reactor was operated at room temperature, in single-pass continuous mode, using liquids flows of 7 ml min<sup>-1</sup> for the single tubes and 100 ml min<sup>-1</sup> for multichannels. 0.1 mol/l formic acid solution was used as an effluent. The conversion of organic molecules was monitored using a Shimadzu TOC 5050A total organic carbon analyser. The reaction rate was expressed as carbon moles converted per unit time, related to the geometric membrane area. As a matter of fact, the membrane area is the cost-limiting factor of this process.

### 5.3. Performance results

Fig. 7 shows the observed reaction rates, as a function of the type of membrane and the gas overpressure. Two main trends can be seen: (i) the gas overpressure strongly enhances the reactor performance, and (ii) the performance is globally higher on single tubes than on multichannel systems.

The influence of the gas pressure was attributed to its effect on the gas–liquid location within the membrane wall rather than to kinetic order effect [43]. This can be seen when comparing results on samples a and b. Due to the presence of only three layers, the membrane a performance shows a important change when moving from 3.6 to 5 bar overpressure. This is not the case of membrane b, as the same pressure change cannot push the gas/liquid interface further than the third layer (see the pore size of the different layers in Table 1). In the case of membrane c, the pore size distribution between layers is slightly different, but, more importantly, the catalyst support material itself (ceria-doped zirconia) plays an important role in improving the kinetics [44].

The scale-up of this process implied transferring the catalyst membrane implementation to multichannel systems. It can be observed from the above results that, whereas the trend between the different membrane materials is conserved, the overall

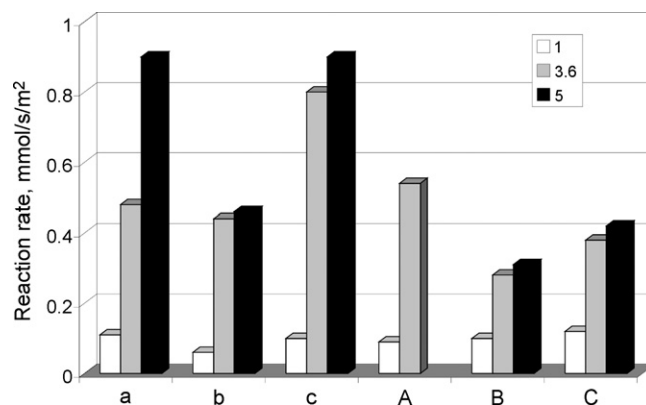


Fig. 7. Oxidation rate as a function of catalytic membrane material at 3 different gas overpressures [a–c: single tubes, A–C: multichannels].

performance is reduced on such material. This can be attributed to differences in the catalyst distribution between the channels during deposition [42].

As a conclusion to this part, one can note that the performance of this CMR for oxidation of wastewaters motivated the development of a pilot unit, now in testing operation on industrial effluents in Norway, under the responsibility of Due Miljø [45].

## 6. Conclusion

The examples of catalytic membrane reactors presented here cover a wide range of applications from synthesis industrial processes to environmental remediation applications. These reactors can be operated in many different modes, using various membrane materials. Beside adapted membranes, catalysts must be tuned to fit into the system and match the constraints and specific operational conditions of membrane catalysis. For all applications presented in this paper, an enhancement in the performance of the reactor was observed, over their conventional counterparts. However, these advantages differ from one system to another one.

In the case of butane to maleic anhydride, the productivity is increased because the distribution allows much higher butane feeds, while keeping safe operation. For propane to propene, the oxygen partial pressure control favours the primary alkene production, leading to higher selectivities at constant conversion. In both cases, the membrane reactor could take benefit of a transient operation mode.

Ethane dehydrogenation to ethylene in a dense ionic oxygen conducting membrane reactor offers a new way to feed activated oxygen species to the catalyst (VMgO or Pd based), leading yields significantly over the industrial conventional processes.

The membrane reactor provides wet air oxidation with a large increase of reaction rate when compared to conventional reactors. This can be finely monitored according to the membrane structure and operational conditions that control the gas–liquid interface location.

The two last applications are still the subject of intensive research in our group. In particular, the change of membrane design, where hollow fibre-type geometry could present a decisive breakthrough is under investigation.

## References

- [1] J. Sanchez, T.T. Tsotsis, *Catalytic Membranes and Membrane Reactors*, VCH Verlag GmbH, Weinheim, 2002.
- [2] S. Mota, S. Miachon, J.-C. Volta, J.-A. Dalmon, *Catal. Today* 67 (2001) 169–176.
- [3] J.N. Armor, *J. Membr. Sci.* 147 (1998) 217–233.
- [4] J. Caro, T. Schiestel, S. Werth, H. Wang, A. Kleinert, P. Kolsch, *Desalination* 199 (2006) 415–417.
- [5] A. Lofberg, H. Bodet, C. Pirovano, M.C. Steil, R.N. Vannier, E. Bordes-Richard, *Catal. Today* 118 (2006) 223–227.
- [6] T. Nozaki, O. Yamasaki, K. Omata, K. Fujimoto, *Chem. Eng. Sci.* 47 (1992) 2945–2950.
- [7] K. Omata, S. Hashimoto, H. Tominaga, K. Fujimoto, *Appl. Catal.* 52 (1989) L1–L4.
- [8] C. Tellez, M. Menendez, J. Santamaria, *Chem. Eng. Sci.* 54 (1999) 2917–2925.
- [9] V.T. Zaspalis, W. Van Praag, K. Keizer, J.G. Van Ommen, J.R.H.B. Ross, A.J. Fac, *Appl. Catal. B* 74 (1991) 205–222.
- [10] M. Abon, J. Volta, *J. Phys. Chem.* 157 (1997) 173–193.
- [11] R. Mallada, M. Menéndez, J. Santamaría, *Catal. Today* 56 (2000) 191–197.
- [12] E. Xue, J. Ross, *Catal. Today* 61 (2000) 3–8.
- [13] S. Miachon, E. Landrison, M. Aouine, Y. Sun, I. Kumakiri, Y. Li, et al. *J. Membr. Sci.* 281 (2006) 228–238.
- [14] S. Mota, J.C. Volta, G. Vorbeck, J.A. Dalmon, *J. Catal.* 193 (2000) 319–329.
- [15] A. Cruz-López, N. Guilhaume, S. Miachon, J. Dalmon, *Catal. Today* 107–108 (2005) 949–956.
- [16] O. Pachtová, I. Kumakiri, M. Kocirik, S. Miachon, J. Dalmon, *J. Membr. Sci.* 226 (2003) 101–110.
- [17] S. Mota, M. Abon, J.C. Volta, J. Dalmon, *J. Catal.* 193 (2000) 308–318.
- [18] J. Millet, *Top. Catal.* 38 (2006) 83–92.
- [19] M. Char, D. Patel, H.H. Kung, *J. Catal.* 109 (1988) 463.
- [20] A. Pantazidis, A. Auroux, J.M. Herrmann, C. Mirodatos, *Catal. Today* 32 (1996) 81–88.
- [21] A. Pantazidis, A. Burrows, C.J. Kielly, C. Mirodatos, *J. Catal.* 177 (1998) 325–334.
- [22] A. Pantazidis, S.A. Buchholz, H.W. Zanthoff, Y. Schuurman, C. Mirodatos, *Catal. Today* 40 (1998) 207–214.
- [23] H.W. Zanthoff, S.A. Buchholz, A. Pantazidis, C. Mirodatos, *Chem. Eng. Sci.* 54 (1999) 4397–4405.
- [24] C. Téllez, M. Abon, J.A. Dalmon, C. Mirodatos, J. Santamaría, *J. Catal.* 195 (2000) 113–124.
- [25] A. Julbe, D. Farrusseng, J.C. Jolibert, C. Mirodatos, C. Guizard, *Catal. Today* 56 (2000) 199–209.
- [26] D. Creaser, B. Andersson, R.R. Hudgins, P.L. Silveston, *Chem. Eng. Sci.* 54 (1999) 4437–4448.
- [27] H. Zanthoff, J.C. Jolibert, Y. Schuurman, J.M. Herrmann, C. Mirodatos, *Studies in Surf. Sci. Catal.* 130A (2000) 761–766.
- [28] Y. Liu, P. Cong, R. Doolen, S. Guan, V. Markov, L. Woo, et al. *J. Phys. Chem.* 254 (2003) 59.
- [29] F. Akin, Y. Lin, *J. Membr. Sci.* 209 (2002).
- [30] H. Wang, Y. Cong, W. Yang, *Catal. Lett.* 84 (2002) 101.
- [31] D. Farrusseng, A.C. van Veen, M. Rebeilleau, C. Mirodatos, S. Rushworth, *French Patent* 03 102 58, 2003.
- [32] Z. Shao, H. Dong, G. Xiong, C. You, W. Yang, *J. Membr. Sci.* 183 (2001) 181.
- [33] Z. Shao, G. Xiong, H. Dong, W. Yang, L. Lin, *Sep. Purif. Technol.* 25 (2001) 97.
- [34] A.C. van Veen, M. Rebeilleau, D. Farrusseng, C. Mirodatos, *Chem. Com.* 32 (2002) 32.
- [35] J.L. Rousset, A.J. Renouprez, A.M. Cadrot, *Phys. Rev. B-Cond. Matter* 58 (1998) 2150.
- [36] M. Rebeilleau-Dassonneville, S. Rosini, A.C. van Veen, D. Farrusseng, C. Mirodatos, *Catal. Today* 104 (2005) 131–137.
- [37] E.E. Iojoiu, S. Miachon, J. Dalmon, *Top. Catal.* 33 (2005) 135–139.
- [38] S. Miachon, V. Perez, G. Crehan, E. Torp, H. Ræder, R. Bredesen, J.-A. Dalmon, *Catal. Today* (2003) 75–81.
- [39] G. Bercic, A. Pintar, J. Levec, *Catal. Today* 105 (2005) 589–597.
- [40] P. Cini, M.P. Harold, *AIChE J.* 37 (1991) 997–1008.
- [41] J. Peureux, M. Torres, H. Mozzanega, A. Giroir-Fendler, J.-A. Dalmon, *Catal. Today* 25 (1995) 409–415.
- [42] E.E. Iojoiu, S. Miachon, E. Landrison, J. Walmsley, H. Raeder, J. Dalmon, *Appl. Catal. B* 69 (2006) 196–206.
- [43] E.E. Iojoiu, J.C. Walmsley, H. Raeder, S. Miachon, J. Dalmon, *Catal. Today* 104 (2005) 329–335.
- [44] J. Barbier, G. Blanchard, F. Delanoe, D. Duprez, P. Isnard, *French Patent* 2 750 976 (1996).
- [45] E.E. Iojoiu, E. Landrison, H. Raeder, E.G. Torp, S. Miachon, J. Dalmon, *Catal. Today* 118 (2006) 246–252.